DOI: 10.1002/chem.201300588

Aptamer-Based Turn-On Detection of Thrombin in Biological Fluids Based on Efficient Phosphorescence Energy Transfer from Mn-Doped ZnS Quantum Dots to Carbon Nanodots

Lu Zhang, Peng Cui, Baocheng Zhang, and Feng Gao*[a]

Abstract: This paper presents the first example of a sensitive, selective, and stable phosphorescent sensor based on phosphorescence energy transfer (PET) for thrombin that functions through thrombin–aptamer recognition events. In this work, an efficient PET donor–acceptor pair using Mn-doped ZnS quantum dots labeled with thrombin-binding aptamers (TBA QDs) as donors, and carbon nanodots (CNDs) as acceptors has been constructed. Due to the π–π stacking interaction between aptamer and CNDs, the energy donor and acceptor are taken into close proximity, leading to the phosphorescence quenching of donors, TBA QDs. A maximum phosphorescence quenching efficiency as high as 95.9% is acquired. With the introduction of thrombin to the "off state" of the TBA-QDs-CNDs system, the phosphorescence is "turned on" due to the formation of quadruplex-thrombin complexes, which releases the energy acceptor CNDs from the energy donors. Based on the restored phosphorescence, an aptamer-based turn-on thrombin biosensor has been demonstrated by using the phosphorescence as a signal transduction method. The sensor displays a linear range of 0–40 nM for thrombin, with a detection limit as low as 0.013 nM in pure buffers. The proposed aptasensor has also been used to monitor thrombin in complex biological fluids, including serum and plasma, with satisfactory recovery ranging from 96.8 to 104.3%. This is the first time that Mn-doped ZnS quantum dots and CNDs have been employed as a donor–acceptor pair to construct PET-based biosensors, which combines both the photophysical merits of phosphorescence QDs and the superquenching ability of CNDs and thus affords excellent analytical performance. We believe this proposed method could pave the way to a new design of biosensors using PET systems.

Keywords: aptamers · biosensors · quantum dots · phosphorescence · energy transfer

Introduction

The development of sensitive, selective, and cost-effective methods for the detection of disease-related biomolecules in biological fluids has attracted much attention because of their potential applications in clinical diagnostics and treatment. Human α-thrombin (thrombin), a trypsin-like serine protease that converts soluble fibrinogen into insoluble strands of fibrin and catalyzes many other coagulation-related reactions, plays important roles in molecular biology, such as in the regulation of tumor growth, metastasis, and angiogenesis.[1] Clearly, it is of great importance to establish highly sensitive and selective methods to detect thrombin. Among the developed approaches for thrombin detection, aptamer-based thrombin biosensors (known as aptasensors or aptamer beacons) that exploit thrombin-binding aptamer (denoted as TBA, e.g., 15-mer, 5-GGTTGGTGTGGTTGG-3) as a biorecognition element and then transduce the binding-induced conformational changes into a quantifiable signal, have been extensively investigated because of the high specificity of protein–aptamer recognition events.[2–11] For most of these aptamer-based thrombin sensors, the signal transduction methods rely on electrochemical and optical schemes. Electrochemical signal transduction methods include amperometric,[3] and impedimetric signaling.[4] Optical signal transduction methods include fluorescence,[5] absorbance,[6] electrochemiluminescence,[7] mass spectroscopy,[8] surface enhanced resonance Raman scattering (SERRS),[9] and localized surface plasmon resonance (LSPR).[10] Recently, the Kopelman group has presented label-acquired magnetorotation (LAM) for thrombin detection as a new signal transduction method.[11]

Room-temperature phosphorescence (RTP) can be defined as radiative transition originating from the lowest excited triplet state, T_1, to the ground singlet state, S_0. As a very useful signal transduction method, RTP has gained significance for optical sensing applications because it displays many advantages over steady-state fluorescence methods. Especially, the longer emission lifetime of the triplet excited state of phosphors allows an appropriate delay time so that any fluorescent emission and scattering light can be easily

[a] L. Zhang, P. Cui, B. Zhang, Prof. F. Gao
Laboratory of Optical Probes and Bioelectrocatalysis (LOPAB)
Anhui Key Laboratory of Chemo/Biosensing
College of Chemistry and Materials Science
Anhui Normal University, Wuhu 241000 (P.R. China)
Fax: (+86) 553-3869302
E-mail: fgao@mail.ahnu.edu.cn

Supporting information for this article is available on the WWW under http://dx.doi.org/10.1002/chem.201300588.

avoided. Furthermore, RTP detection is a more efficient approach for elimination of background fluorescence in complex matrixes (e.g., environmental samples, foods, and biological fluids).[12–14] Despite the advantages offered by RTP detection, its most important drawback, which limits the development of new RTP-sensing systems, is the lack of suitable phosphorescence indicators for a given analyte. However, phosphorescence energy transfer (PET), a long range and nonradiative energy transfer process in which the phosphorescent molecule (donor) transfers its energy to the absorber (acceptor) within close proximity through dipole–dipole coupling of the donor and acceptor molecules, could be used as a general strategy to develop RTP-sensing schemes.[12] In the few FET-based analytical systems that have been developed,[15] the mechanism is based on the concept of converting color changes into luminescence emission information. Provided that there is spectral overlap of the absorption spectrum of an analyte-dependent dye acceptor with the emission of an inert phosphorescent donor, the donor (phosphorescent molecule) transfers its energy to the acceptor (analyte-sensitive dye) and the acceptor dissipates this energy through nonradiative processes. Based on the color changes of analyte-dependent dye acceptor, which will change the phosphorescence intensity of the donor, a FET method for determination of the analyte can be developed.

In the present study, a novel PET-based analytical system with high sensitivity and specificity has been designed. In the designed PET model, a donor–acceptor pair is constructed and can be brought to a suitable distance to make PET occur, which "turns off" the phosphorescence of the donor. When the analyte is introduced into the system, the phosphorescence of the donor is "turned on" due to the specific intermolecular recognition event between the analyte and donor, which makes the acceptor release from the donor. Based on the restored phosphorescence, a PET-based detection method for the analyte can be proposed. However, to the best our knowledge, such attempts have not so far been made to design biosensors. Herein, we demonstrate the first example of a sensitive, selective, and stable PET-based phosphorescent sensor for thrombin that functions through a thrombin–aptamer recognition event.

In the proposed PET system, Mn-doped ZnS quantum dots (Mn-ZnS QDs) and carbon nanodots (CNDs) are used as energy donors and acceptors, respectively. Recently, Mn-ZnS QDs have attracted considerable interest and have been used as promising room-temperature phosphorescence probes for optosensors due to the long-lived RTP emission of Mn-ZnS QDs that allows autofluorescence and scattering light to be avoided.[14] In another aspect, QDs have shown many advantages over conventional organic dyes and inorganic luminophors such as high quantum yield, tunable emission wavelength, and good resistance to photobleaching. Water-soluble QDs are also easy for bioconjugation and are widely employed as chemo/biosensing materials.[16] To design an efficient PET system in which energy acceptors could quench the emission of donors as much as possible, the choice of acceptors with strong quenching ability is of great importance because a larger quenching efficiency will generally lead to higher detection sensitivity in quantitative assays.[5l,17] Recently, graphite-based structures (e.g., graphene or grapheme oxide) with sp^2 electronic hybrid and a large conjugate plane have exhibited superquenching ability and have been employed as energy acceptors, which may be attributed to their strong electron-capturing tendency.[5j,m,18] Carbon nanodots (CNDs), a newly emerging form of carbon nanomaterials with the size of zero-dimension, have inspired intense research efforts in various fields, such as bioimaging and light energy conversion.[19] CNDs possess similar sp^2 electronic structure to that of graphene, and broad absorption bands, which means they are expected to possess strong phosphorescence quenching ability and are favorable candidates for energy acceptors. However, the use of CNDs as energy acceptors has rarely been reported.[5l]

In the present work, we have developed a PET-based biosensor using Mn-ZnS QDs and CNDs as the energy donor–acceptor pair for the first time. The strategy for thrombin detection is based on aptamer-bridged phosphorescent energy transfer from Mn-ZnS QDs to CNDs, as shown in Scheme 1. In our design, energy donors Mn-ZnS QDs are

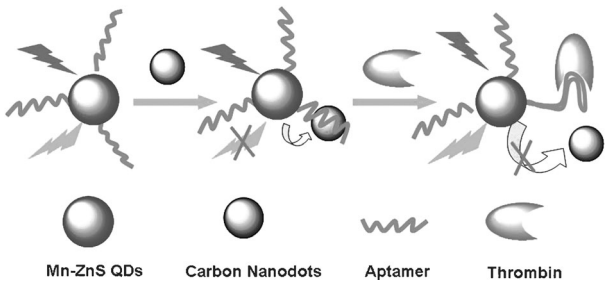

Scheme 1. Schematic illustration of the turn-on thrombin sensor based on PET from aptamer-labeled Mn-ZnS QDs to carbon nanodots.

first labeled with thrombin-binding aptamers (denoted as TBA QDs), on the basis of the π–π interaction between the aptamer and CNDs due to the sp^2 electronic hybrid structure of CNDs, the donor and the acceptor are taken into close proximity, which results in the occurrence of PET and phosphorescence quenching of TBA QDs (off-state). With the introduction of target analyte, thrombin, to the as-formed TBA-QDs-CNDs system, the formation of quadruplex-thrombin complex will lead to the disappearance of the π–π stacking interaction, thus CNDs are released from the TBA QDs. As a result, the PET process is inhibited and the phosphorescence of TBA QDs is recovered (turn-on state). Based on the restored phosphorescence, a homogeneous turn-on assay for thrombin is proposed.

Results and Discussion

Characterization of MPA-capped Mn-doped ZnS QDs and carbon nanodots: To realize the above PET couple, 3-mercaptopropionic acid (MPA) capped Mn-Doped ZnS QDs

(MPA QDs) and carbon nanodots were first synthesized and characterized, respectively. The synthesis of MPA QDs was carried out through the reaction of zinc sulfate, manganese chloride, and sodium sulfide, according to a previously reported procedure.[14c,20] In the present synthesis, the introduction of MPA can greatly improve the efficiency and reproducibility of the doping of Mn due to the covalent interaction between thiols and the surface of the QDs.[20] Furthermore, conjugation of the thrombin aptamer with MPA QDs can be achieved with the aid of coupling reagents, 1-ethyl-3-(3-dimethyllaminopropyl) carbodiimide (EDC) and *N*-hydroxysuccinimide (NHS).[17a] The morphologies of the MPA QDs were observed by transmission electron microscopy (TEM), as shown in Figure 1 A. The particles show spherical shape and have nearly uniform size. A little agglomeration is observed due to the evaporation of solvent. The average diameter of these nanocrystals is estimated to be 3.0 nm. These observed characterizations are in good agreement with previous publications.[14c,20] The thrombin aptamer was conjugated to MPA QDs through the use of conventional coupling reagents, EDC and NHS, followed by purification with an ultrafilter membrane. Figure 1 B displays the UV/Vis absorption spectra of MPA-QDs-aptamer conjugates (TBA QDs), a characteristic absorption peak located at approximately 260 nm for the protein was observed, indicating that the aptamer was successfully connected to the MPA QDs.

A typical SEM image of the acceptor, that is, carbon nanodots (CNDs), is shown in Figure 1 C. It is clear that the CNDs are uniform in size, with a diameter of about 50 nm. Figure 1 D shows the UV/Vis absorption spectrum of the as-prepared CNDs, which consists of a peak (ca. 280 nm) and a strong background that extends to 700 nm. It is generally accepted that the peak and the background extinction are known to occur for CNDs although the exact assignment of the peak is still unclear.[19b–f] The broad absorption band spanning a wide range of wavelengths makes CNDs possible energy acceptors for a variety of donors.

PET between TBA QDs and CNDs: Figure S1 (see the Supporting Information) shows the absorption spectrum of CNDs and the phosphorescence emission spectrum of TBA QDs, respectively. It can be seen that the emission spectrum of TBA QDs overlap with the absorption spectrum of CNDs to an extent, suggesting that PET between them can take place. According to the PET process, in this system TBA QDs act as donors, while CNDs act as acceptors (quenchers).[12]

To further confirm the PET, we investigated the emission spectra of TBA QDs in the presence of different concentrations of CNDs. As shown in Figure 2 A, the phosphorescence intensities of TBA QDs at a fixed concentration of 0.03 mg mL^{-1} decreased gradually with increasing concentration of CNDs ranging from 0.0 to 0.045 mg mL^{-1}, and the maximum quenching was observed at 0.045 mg mL^{-1} CNDs. This result indicates that when CNDs were introduced into TBA QDs solution, the energy was transferred from TBA QDs to CNDs, resulting in quenching of the phosphorescence of TBA QDs. The quenching efficiency was calculated by $(1-P/P_0)$, in which P_0 and P represent the phosphores-

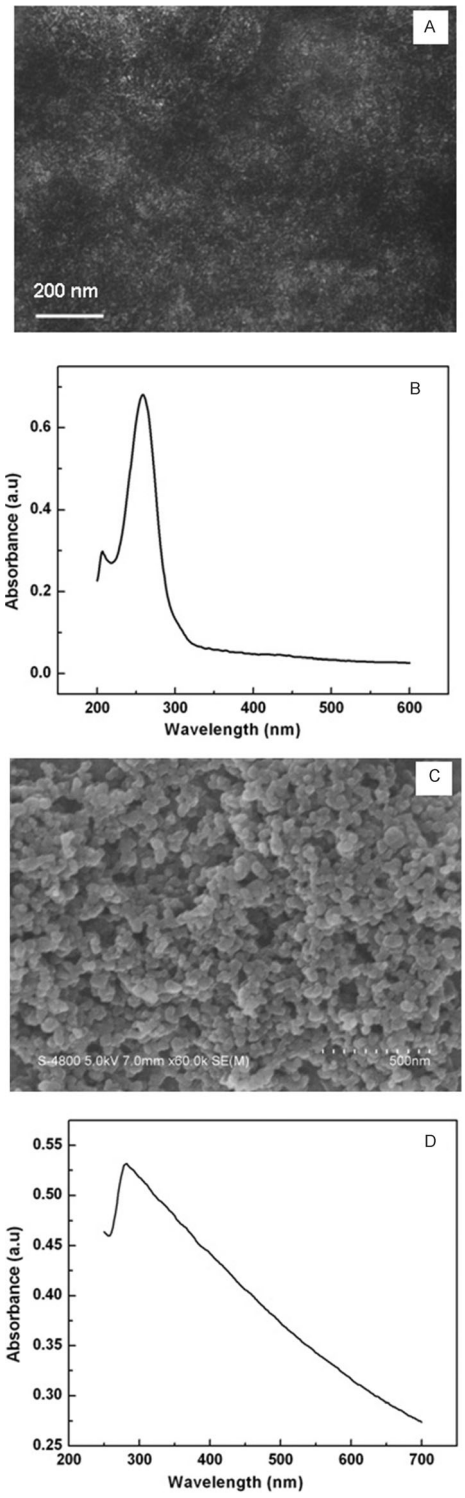

Figure 1. A) Typical TEM image of the MPA-capped Mn-doped ZnS QDs (MPA QDs). B) UV/Vis absorption spectrum of 0.03 mg mL^{-1} MPA QDs labeled with aptamer. C) Typical SEM image of carbon nanoparticles. D) UV/Vis absorption spectrum of the as-prepared carbon nanodots with a concentration of 0.045 mg mL^{-1}.

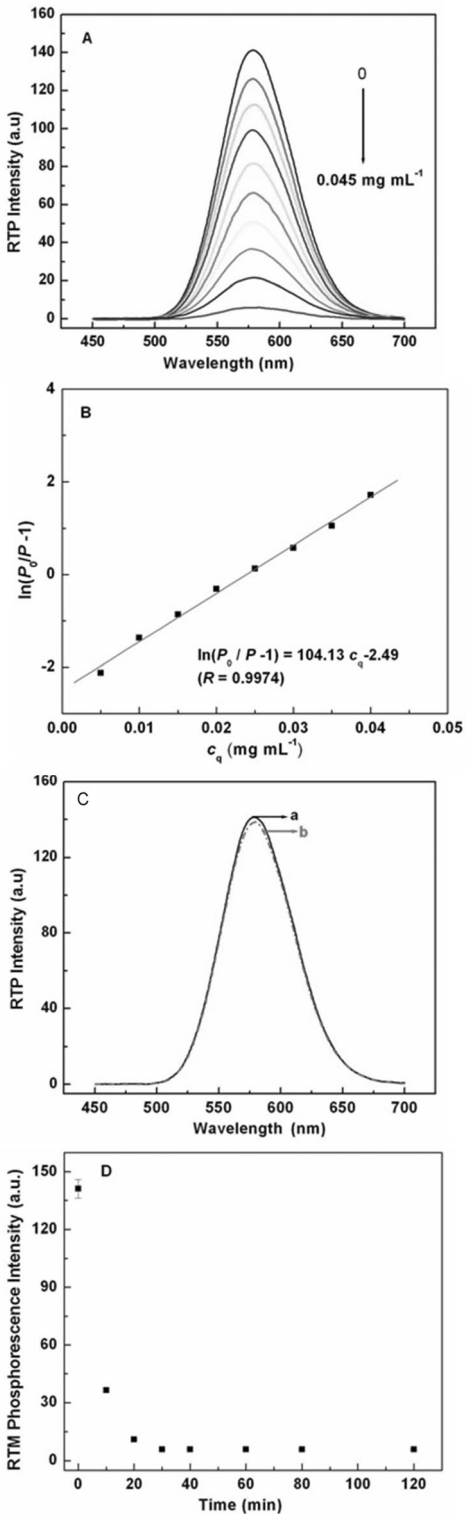

Figure 2. A) Phosphorescence quenching of TBA QDs with varying amounts of CNDs. TBA QDs: 0.03 mg mL^{-1}; CNDs from top to bottom: 0, 0.005, 0.01, 0.015, 0.02, 0.025, 0.03, 0.035, 0.04, 0.045 mg mL^{-1}. B) Plot of phosphorescence intensity of TBA QDs versus CNDs concentration based on an empirical equation. The data are obtained from A). C) Phosphorescence spectra of MPA QDs in the absence (curve a, solid line) and presence (curve b, dashed line) of 0.045 mg mL^{-1} CNDs. D) Time dependence of phosphorescence quenching of 0.03 mg mL^{-1} TBA QDs by 0.045 mg mL^{-1} CNDs. All experiments were performed in Tris/HCl buffer (0.01 M, 0.15 M NaCl, pH 7.4) under excitation at 316 nm.

cence intensity of TBA QDs in the absence and presence of CNDs, respectively, and a maximum quenching efficiency of up to 95.9% was obtained when 0.045 mg mL^{-1} CNDs was introduced. Such a quenching efficiency reveals the superquenching ability of CNDs. This large quenching efficiency largely turns off the phosphorescence of TBA QDs and provides an optimal off-state for a sensitive turn-on quantitative assay.

The phosphorescence quenching is usually divided into static quenching and dynamic quenching. The dynamic quenching can be described by Stern–Volmer's equation [Eq. (1)], whereas the static quenching can be described by the Lineweaver–Burk equation [Eq. (2)] as follows:[12,14a]

$$P_0/P = 1+K_{SV} \times c_q \quad (1)$$

$$1/(P_0-P) = 1/P_0+K_{LB}/(P_0\ c_q) \quad (2)$$

in which P_0 and P represent the relative phosphorescence intensity of TBA QDs in the absence and presence of CNDs, respectively, and c_q is the concentration of the quencher (CNDs). K_{SV} is the dynamic quenching constant, and K_{LB} is the static quenching constant. The plot of the relationships between $1/(P_0-P)$ and $1/c_q$, and P_0/P and c_q are shown in Figure S2A and Figure S2B, respectively (see the Supporting Information). Interestingly, at low concentration of the quencher, the phosphorescence quenching of TBA QDs by CNDs not only follow Stern–Volmer's equation but also the Lineweaver–Burk equation, whereas at high concentration of quencher, the phosphorescence quenching only follows the Lineweaver–Burk equation. These results may indicate that both the dynamic and static quenching seem to act together, suggesting a more complex quenching model. Based on previous reports,[21] an empirical equation could be fitted. As shown in Figure 2B, a linear relationship between $\ln(P_0/P-1)$ and c_q and the equation can be fitted as [Eq. (3)]:

$$\ln(P_0/P-1) = 104.13\ c_q-2.49\ (R = 0.9974) \quad (3)$$

Previous studies have illustrated that the π–π stacking interaction could take place between single-stranded DNA and π electron-rich carbon material such as graphene and carbon nanodots.[5l,22] In the present system, the formation of a nonphosphorescence ground-state complex between the TBA QDs and CNDs can be ascribed to π–π stacking between the aptamer and CNDs.

A control experiment was also performed to investigate nonspecific phosphorescence quenching of MPA QDs (no aptamer labeled). As shown in Figure 2C, with an identical incubation procedure, the phosphorescence did not show a clear change when 0.045 mg mL^{-1} CNDs was introduced. This observation indicates that the nonspecific interaction between MPA QDs and CNDs can be neglected, and that the phosphorescence quenching of TBA QDs can mainly be attributed to aptamer-bridged PET from the donor to ac-

ceptor, as a result of the π–π stacking between the aptamer and CNDs.

Figure 2D shows the time dependence of phosphorescence quenching of TBA QDs by 0.045 mg mL^{-1} CNDs. The phosphorescence quenching of TBA QDs was achieved within approximately 20 min incubation, and a plateau was observed after further reaction time. To ensure complete quenching and obtain a stable signal, an incubation of 30 min was adopted in this step.

Phosphorescence turn-on detection of thrombin based on PET: The effect of thrombin on the PET system of TBA-QDs-CNDs has been investigated. Figure 3A depicts the

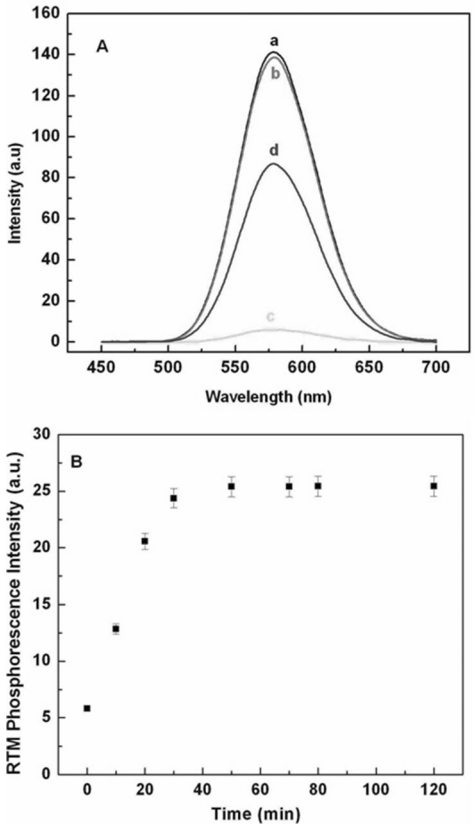

Figure 3. A) Phosphorescence spectra of 0.03 mg mL^{-1} TBA QDs (a), a+20 nM thrombin (b), a+0.045 mg mL^{-1} CNDs (c), and c+20 nM thrombin (d). B) Phosphorescence recovery of TBA-QDs-CNDs system by 5 nM thrombin as a function of incubation time. TBA QDs: 0.03 mg mL^{-1}; CNDs: 0.045 mg mL^{-1}.

emission spectra of TBA QDs, TBA-QDs-thrombin, TBA-QDs-CNDs, and TBA-QDs-CNDs-thrombin under the same experimental conditions. As shown in this figure, TBA QDs exhibits a strong phosphorescence signal at approximately 581 nm (curve a), and its phosphorescence intensity and peak location do not change significantly when 20 nM thrombin was added to the solution (curve b). When CNDs was added into the TBA QDs solution, the phosphorescence intensity of TBA QDs decreased due to the FET process between TBA QDs and CNDs (curve c). Upon addition of 20 nM thrombin into the TBA-QDs-CNDs solution, the phosphorescence of the TBA-QDs-CNDs system was restored (curve d). These results suggest that with the addition of free thrombin to the TBA-QDs-CNDs PET system, the aptamer was induced to from quadruplex-thrombin structure due to the binding of thrombin to TBA QDs through an aptamer-target affinity interaction, which dramatically weakened the π–π interaction between aptamers and CNDs. Therefore, the energy acceptors, CNDs were separated away from the donors, resulting in the restoration of the phosphorescence of energy donors, TBA QDs. Based on the restored phosphorescence, a phosphorescent turn-on method for the determination of thrombin was proposed.

The effect of incubation time on phosphorescence recovery of the TBA-QDs-CNDs PET system was also investigated by collecting time-independent phosphorescence emission spectra. As shown in Figure 3B, after addition of 5 nM thrombin to the TBA-QDs-CNDs system, the phosphorescence signal increases quickly and phosphorescence was restored to the maximal extent within approximately 40 min and thereafter remained quite stable. Therefore, reaction times of 40 min for phosphorescence recovery were used.

Under the optimum experimental conditions, the analytical parameters for the determination of thrombin were evaluated in pure buffer. Figure 4A displays the phosphorescence recovery of the TBA-QDs-CNDs PRET system in the presence of varying concentrations of thrombin. As shown in this figure, with increasing concentration of thrombin, the phosphorescence intensity of TBA-QDs-CNDs PET system increased gradually. The plot of the phosphorescence enhanced efficiency, defined as $(P-P_0)/P_0$ (P and P_0 represent the phosphorescence intensity in the presence of different concentrations of thrombin and absence of thrombin, respectively), against the concentration of added thrombin is also shown in Figure 4B. It is clear that the phosphorescence enhanced efficiency exhibits a linear response to the thrombin concentration in the range from 0 to 40 nM, with a correlation coefficient of 0.9958, and the calibration curve can be expressed as $(P-P_0)/P_0=0.8356+0.5639c$ (c in nM). The limit of detection (3σ) for thrombin is 0.013 nM, in which σ represents the standard deviation of eight blank measurements.[23] These analytical parameters are better or favorably comparable to those reported in literature, as shown in Table S1 (see the Supporting Information). The performance of these analytical techniques, including the low detection limit, can be attributed to a combination of the advantages of the phosphorescence method and the specific interaction of the aptamer-protein. The repeatability of the proposed methods was also evaluated by measurements of 5 nM thrombin, and the relative standard deviation for seven repeated measurements was found to be 4.37%, indicating that the response of the TBA-QDs-CNDs PET system to thrombin is highly reproducible.

Cross-reactivity of the PET-based aptamer sensor for thrombin: To evaluate the specificity of the PET-based aptasensor for thrombin, the influence of potentially interfering sub-

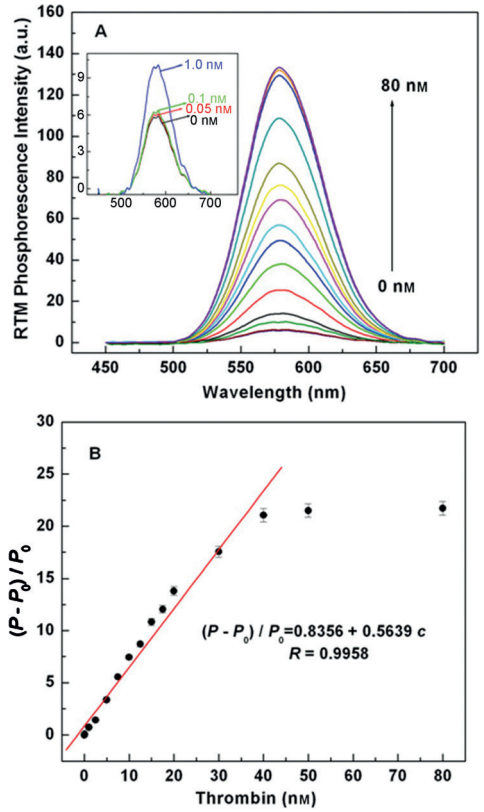

Figure 4. A) Phosphorescence recovery of aptamer sensor with various concentrations of thrombin. From bottom to top: 0, 0.05, 0.1, 1.0, 2.5, 5.0, 7.5, 10.0, 12.5, 15.0, 17.5, 20.0, 30.0, 40.0, 50.0, 80.0 nM. Inset shows the enlarged curve in the low thrombin concentration range. B) Plot of the phosphorescence recovery as a function of concentration of thrombin. Each data point represents the average value of three independent experiments with error bars indicated. All experiments were performed in Tris/HCl buffer (0.01 M, 0.15 M NaCl, pH 7.4) in the presence of 0.03 mg mL^{-1} TBA QDs and 0.045 mg mL^{-1} CNDs.

stances including proteins and common ions were investigated under the same experimental conditions. We investigated the phosphorescence intensity of the TBA-QDs-CNDs PET system to thrombin in the presence of different interfering substances. As shown in Figure 5, the relative phosphorescence intensity P/P_0 (in which P_0 and P is the phosphorescence intensity of the aptasensor without and with interfering species and thrombin, respectively) of the biosensor in the presence of 5 nM thrombin is 4.54, which is much higher than that of other interfering species at a concentration as high as 1.0 μM. These results indicate that the phosphorescence of the aptasensor changed less for the interfering species, whereas a significant phosphorescence increase was observed for thrombin. The good selectivity of the PET aptasensor is attributed to the high specificity of the aptamer. Therefore, the PET aptasensor possesses a good selective phosphorescence response toward thrombin, and also indicated that a turn-on phosphorescent method for the determination of thrombin could be developed with the present system.

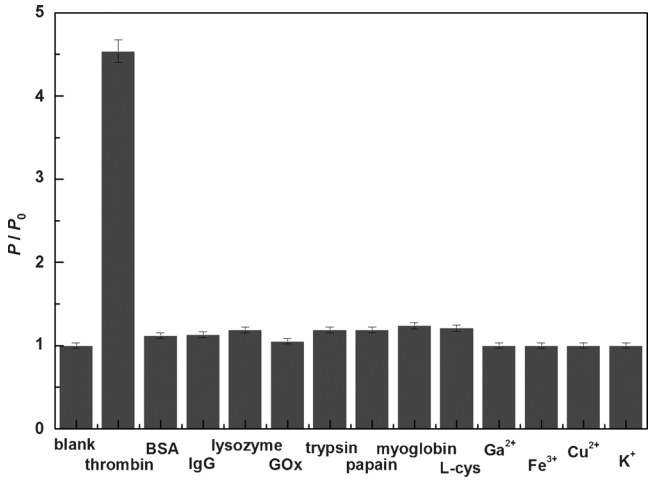

Figure 5. Selectivity of the aptasensor for thrombin detection by comparison with common potentially interfering species. The concentration of all interfering species was 1.0 μM and thrombin concentration was 5 nM. Relative phosphorescence intensity (P/P_0) was calculated by P/P_0 in which P_0 and P are the phosphorescence intensity without and with interfering species and thrombin, respectively. Experiments were performed in Tris/HCl buffer (0.01 M, 0.15 M NaCl, pH 7.4) under excitation at 361 nm, in the presence of 0.03 mg mL^{-1} TBA QDs and 0.045 mg mL^{-1} CNDs.

Thrombin analysis in biological fluids with the aptamer sensor: To verify the practical applications of the proposed PET-based phosphorescent aptasensor, the ability of the aptasensor to detect thrombin in complex biological fluids including human serum and plasma was evaluated.

Human serum: Serum is what remains from whole blood after coagulation. Because no coagulation factors are contained in healthy human serum sample, no thrombin exists in the serum sample. In this study, serum samples were obtained from healthy persons. Prior to use, serum was diluted tenfold with Tris/HCl buffer and tested either alone or spiked with standard solutions of thrombin. Figure 6A displays the phosphorescence recovery of aptasensor with various concentrations of thrombin in human serum. It is clear that addition of thrombin to the serum sample also resulted in a concentration-dependent signal. As shown in Figure 6B, a linear range for thrombin was also obtained in the range from 0 to 40 nM, with a correlation coefficient of 0.9991, and the linear curve can be described as $(P-P_0)/P_0 = -0.06954+0.1169c$ (c in nM). Compared with the response of the aptasensor in pure buffer, a lower sensitivity for thrombin detection (i.e., the slope of linear regression equation) was observed in serum sample. This decrease can probably be ascribed to the reduced concentration of thrombin available for the binding caused by interactions with some matrix components in serum. The limit of detection (3σ) for thrombin was also measured and found to be 0.048 nM. The repeatability of the aptasensor analytical system in serum was also evaluated by measurements of 5 nM thrombin, and the relative standard deviation for seven repeated measurements was found to be 6.1%, suggesting that the response

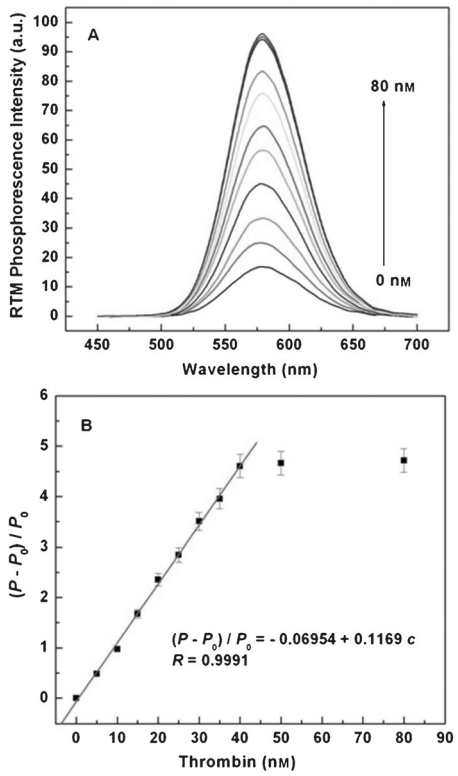

Figure 6. A) Phosphorescence recovery of aptamer sensor with various concentrations of thrombin. From bottom to top: 0, 5.0, 10.0, 15.0, 20.0, 25.0, 30.0, 35.0, 40.0, 50.0, 80.0 nM. B) Plot of phosphorescence recovery as a function of concentration of thrombin. Each data point represents the average value of three independent experiments with error bars indicated. All experiments were performed in serum in the presence of 0.03 mg mL^{-1} TBA QDs and 0.045 mg mL^{-1} CNDs.

of the aptasensor to thrombin in serum is also reproducible. Different concentrations of thrombin were spiked into tenfold-diluted serum samples to examine the applicability of the aptasensor in real serum samples. The serum samples were spiked with 5.0, 10.0, and 20.0 nM thrombin and then measured. The recoveries were obtained by comparing the measured amounts to that of added human thrombin; the results are summarized in Table 1. The recoveries varied from 97.8 to 104.1%, suggesting that the PET-based phosphorescent aptasensor may be competent for monitoring thrombin in real samples.

Table 1. Recovery of thrombin assay at different concentrations spiked into human serum and plasma samples.[a]

Sample[b]	Measured [nM]	Spiked [nM]	Found [nM±SD]	Recovery [%]
1	–[c]	5.0	4.89±0.02	97.8±0.4
2	–[c]	10.0	10.41±0.03	104.1±0.3
3	–[c]	20.0	20.33±0.05	101.7±0.3
4	3.7	10	13.58±0.01	96.8±0.3
5	1.9	10	11.87±0.04	98.4±0.2
6	2.3	10	12.40±0.02	104.3±0.1

[a] All human serum and plasma samples were diluted tenfold prior to assay. Measurements on each sample were repeated five times. [b] Samples 1–3 were serum samples from healthy people and samples 4–6 were plasma samples. [c] Not detectable.

Human plasma: Generally, plasma is composed of 90% water and 10% solutes including prothrombin, fibrin and fibrinogen, coagulation cofactors, and organic compounds of low molecular weight.[3e] Thrombin is absent in plasma of healthy subjects when coagulation is not occurring. In this study, thrombin was generated in situ from prothrombin, the precursor of thrombin, by activated factor Xa through a proteolytic process. To avoid clotting, which will deplete thrombin, fibrinogen in plasma was first precipitated quantitatively by the addition of ammonium sulfate.[24] The generation of thrombin in plasma was time-dependent (data not shown). After generation in situ, the plasma samples containing thrombin were obtained and diluted tenfold with Tris/HCl buffer for further use. The samples were incubated with the proposed aptasensor, then the assay was carried out with similar analytical procedures to those used with serum. Three independent plasma samples were tested and the results are shown in Table 1. Using the calibration curve obtained in the human serum matrix, the concentrations of thrombin in three plasma samples were obtained; the values found were consistent with the previous reported levels.[5l] Standard addition experiments were further carried out with these plasma samples to validate the determination. The recoveries ranged from 96.8 to 104.3%, which are acceptable for quantitative assays performed with biological samples.

Conclusion

We have developed a novel phosphorescence energy transfer system using Mn-doped ZnS QDs as donors and carbon nanodots as acceptors, and also demonstrated its application in biosensing for thrombin with a limit of detection of 0.013 nM in solution when using the classic thrombin aptamers as a signal transduction method. The developed PET-based thrombin biosensor has demonstrated favorable analytical performance with complex biological fluids, including serum and plasma, mainly because the interference from autofluorescence and scattering light in complex matrixes can be easily avoided. Such a phosphorescence energy transfer system may pave the way for new designs of chemo/biosensing systems. However, further investigations including detailed mechanisms of phosphorescence energy transfer and the effect of the sizes of Mn-ZnS QDs and carbon nanodots on the energy transfer, are required; these studies are underway in our laboratory.

Experimental Section

Reagents and instrumentation: All chemicals were of analytical grade or better and were used as received without further purification. Thrombin, 1-ethyl-3-(3-dimethyllaminopropyl) carbodiimide hydrochloride (EDC·HCl), 3-mercaptopropionic acid (MPA), sodium dodecyl benzene

sulfonate (SDBS), $ZnSO_4 \cdot 7H_2O$, $Na_2S \cdot 9H_2O$, $MnCl_2 \cdot 4H_2O$, and *N*-hydroxysuccinimide (NHS) were purchased from Sigma–Aldrich. Amine-modified thrombin aptamer (5′-NH_2-GGTTGGTGTGGTTGG-3′) was obtained from Sangon Biotechnology Co., Ltd. (Shanghai, China). All aqueous solutions were prepared by using ultrapure water (Mill-Q, Millipore, 18.2 MΩ resistivity).

Phosphorescence spectra were recorded with an LS-55 fluorescence spectrophotometer (PerkinElmer company, USA) equipped with a quartz cell (1 cm × 1 cm) operating in the phosphorescence mode. Morphological measurements of Mn-ZnS QDs and carbon nanodots were performed with S-4800 field emission scanning electron microscopy (SEM) (Hitachi, Japan) or Hitachi H-600 transmission electron microscopy (TEM) (Tokyo, Japan). A pHS-3C pH meter was used for pH measurements (Shanghai, China). UV/Vis absorption spectra were measured with a UV-3010 spectrophotometer (Hitachi, Japan).

Synthesis of MPA QDs and CNDs, and bioconjugation of MPA QDs with thrombin-binding aptamer (TBA QDs): To label Mn-Doped ZnS QDs with thrombin-binding aptamer, MPA capped Mn-doped ZnS QDs was synthesized in aqueous solution,[14c,20] and the conjugation of Mn-ZnS QDs with thrombin aptamer (TBA QDs) was achieved through the use of conventional protocols involving the coupling reaction between EDC and NHS.[17a] Carbon nanodots (CNDs) were prepared from candle soot as original material.[19a] Further details for the preparation of the above materials are available in the Supporting Information.

Thrombin detection in buffer solution and biological fluids: In a typical PET assay in Tris/HCl buffer, CNDs (0.045 mg mL^{-1}) was added to TBA QDs (0.03 mg mL^{-1}) in Tris/HCl buffer (10 mM, pH 7.4, 150 mM NaCl) and the mixture was incubated at RT for 30 min. Thereafter, various concentrations of thrombin were added to the TBA-QDs-CNDs mixed solution, and the mixture was incubated for another 40 min at RT. The reaction mixture was then subject to phosphorescence measurement with an excitation of 316 nm, and the emission intensity at 581 nm was recorded for quantitative analysis. To examine the specificity of the PET sensor, other biomolecules and ions were added into the TBA-QDs-CNDs system in place of thrombin under the same experimental conditions.

For the detection of thrombin in biological fluids, human serum and plasma samples were used that were newly obtained from healthy subjects (provided by Yijishan Hospital, Wuhu). The serum matrix was diluted tenfold with Tris/HCl buffer, which was then used as the assay medium. Human plasma samples were collected in citrate anticoagulation tubes. Fibrinogen was removed through precipitation and thrombin was generated in situ from prothrombin, the precursor of thrombin, by activated factor Xa through a proteolytic process according to the reported method;[24] further details are given in the Supporting Information. Subsequent incubation and phosphorescence measurement procedures were conducted as described for samples in buffer solution.

Acknowledgements

We are grateful for financial support from the Natural Science Foundation of China (Grant No. 21175002), the Program for New Century Excellent Talents in University (NCET-12-0599), the Anhui Provincial Natural Science Foundation for Distinguished Youth (Grant No. 1108085J09), and the project sponsored by SRF for ROCS, SEM. B.Z. also thanks the financial support for postdoctoral research.

[1] a) S. R. Stone, A. Betz, J. Hofsteenge, *Biochemistry* **1991**, *30*, 9841–9848; b) F. Lamy, F. W. David, *Phys. Rev.* **1954**, *34*, 722–729.

[2] a) L. C. Bock, L. C. Griffin, J. A. Latham, E. H. Vermaas, J. J. Toole, *Nature* **1992**, *355*, 564–566; b) C. A. Holland, A. T. Henry, H. C. Whinna, F. C. Church, *FEBS Lett.* **2000**, *484*, 87–91.

[3] a) Y. Xiao, A. A. Lubin, A. J. Heeger, K. W. Plaxco, *Angew. Chem.* **2005**, *117*, 5592–5595; *Angew. Chem. Int. Ed.* **2005**, *44*, 5456–5459; b) R. Polsky, R. Gill, L. Kaganovsky, I. Willner, *Anal. Chem.* **2006**, *78*, 2268–2271; c) A. E. Radi, J. L. A. Sanchez, E. Baldrich, C. K. O'Sullivan, *J. Am. Chem. Soc.* **2006**, *128*, 117–124; d) J. Zheng, W. Feng, L. Lin, F. Zhang, G. Cheng, P. He, Y. Fang, *Biosens. Bioelectron.* **2007**, *23*, 341–347; e) S. Centi, S. Tombelli, A. Minunni, M. Mascini, *Anal. Chem.* **2007**, *79*, 1466–1473; f) A. Numnuam, K. Y. Chumbimuni-Torres, Y. Xiang, R. Bash, P. Thavarungkul, P. Kanatharana, E. Pretsch, J. Wang, E. Bakker, *Anal. Chem.* **2008**, *80*, 707–712; g) Md. A. Rahman, J. I. Song, M.-S. Won, Y.-B. Shim, *Anal. Chem.* **2009**, *81*, 6604–6611; h) F. Yan, F. Wang, Z. Chen, *Sens. Actuators B* **2011**, *160*, 1380–1385.

[4] Z. Zhang, W. Yang, J. Wang, C. Yang, F. Yang, X. Yang, *Talanta* **2009**, *78*, 1240–1245.

[5] a) R. Nutiu, Y. F. Li, *J. Am. Chem. Soc.* **2003**, *125*, 4771–4778; b) V. Pavlov, B. Shlyahovsky, I. Willner, *J. Am. Chem. Soc.* **2005**, *127*, 6522–6523; c) R. Nutiu, Y. F. Li, *Chem. Eur. J.* **2004**, *10*, 1868–1876; d) M. Levy, S. F. Cater, A. D. Ellington, *ChemBioChem* **2005**, *6*, 2163–2166; e) C. X. Lin, E. Katilius, Y. Liu, J. P. Zhang, H. Yan, *Angew. Chem.* **2006**, *118*, 5422–5427; *Angew. Chem. Int. Ed.* **2006**, *45*, 5296–5301; f) B. L. Li, H. Wei, S. J. Dong, *Chem. Commun.* **2007**, 73–75; g) N. Li, C. M. Ho, *J. Am. Chem. Soc.* **2008**, *130*, 2380–2381; h) Q. Zhao, X. F. Li, Y. Shao, X. C. Le, *Anal. Chem.* **2008**, *80*, 7586–7593; i) Y. Wang, B. Liu, *Langmuir* **2009**, *25*, 12787–12793; j) H. Chang, L. Tang, Y. Wang, J. Jiang, J. Li, *Anal. Chem.* **2010**, *82*, 2341–2346; k) Y. H. Tennico, D. Hutanu, M. T. Koesdjojo, C. M. Bartel, V. T. Remcho, *Anal. Chem.* **2010**, *82*, 5591–5597; l) Y. Wang, L. Bao, Z. Liu, D. Pang, *Anal. Chem.* **2011**, *83*, 8130–8137; m) C. Zhang, Y. Yuan, S. Zhang, Y. Wang, Z. Liu, *Angew. Chem.* **2011**, *123*, 6983–6986; *Angew. Chem. Int. Ed.* **2011**, *50*, 6851–6854; n) S. Yan, R. Huang, Y. Zhou, M. Zhang, M. Deng, X. Wang, X. Weng, X. Zhou, *Chem. Commun.* **2011**, *47*, 1273–1275; o) J. Liu, J. Li, Y. Jiang, S. Yang, W. Tan, R. Yang, *Chem. Commun.* **2011**, *47*, 11321–11323; p) S. Zhu, Z. Liu, L. Hu, Y. Yuan, G. Xu, *Chem. Eur. J.* **2012**, *18*, 16556–16561; q) G. Garai-Ibabe, R. Grinyte, A. Canaan, V. Pavlov, *Anal. Chem.* **2012**, *84*, 5834–5837.

[6] a) V. Pavlov, Y. Xiao, B. Shlyahovsky, I. Willner, *J. Am. Chem. Soc.* **2004**, *126*, 11768–11769; b) H. A. Ho, M. Leclerc, *J. Am. Chem. Soc.* **2004**, *126*, 1384–1387; c) H. Wei, B. L. Li, J. Li, E. K. Wang, S. J. Dong, *Chem. Commun.* **2007**, 3735–3737; d) A. Higuchi, Y. D. Siao, S. T. Yang, P. V. Hsieh, H. Fukushima, Y. Chang, R. C. Ruaan, W. Y. Chen, *Anal. Chem.* **2008**, *80*, 6580–6586; e) T. Li, E. Wang, S. Dong, *Chem. Commun.* **2008**, 3654–3656; f) H. Xu, X. Mao, Q. X. Zeng, S. F. Wang, A. N. Kawde, G. D. Liu, *Anal. Chem.* **2009**, *81*, 669–675; g) N. Deng, Z. Liang, Y. Liang, Z. Sui, L. Zhang, Q. Wu, K. Yang, L. Zhang, Y. Zhang, *Anal. Chem.* **2012**, *84*, 10186–10190.

[7] a) L. Yang, J. Zhu, Y. Xu, W. Yun, R. Zhang, P. He, Y. Z. Fang, *Electroanalysis* **2011**, *23*, 1007–1012; b) J. Wang, Y. Shan, W. W. Zhao, J. J. Xu, H. Y. Chen, *Anal. Chem.* **2011**, *83*, 4004–4011; c) G. Jie, J. Yuan, *Anal. Chem.* **2012**, *84*, 2811–2817.

[8] a) R. R. Abzalimov, P. L. Dubin, I. Kaltashov, *Anal. Chem.* **2007**, *79*, 6055–6063; b) Q. Zhao, X. Lu, C. G. Yuan, X. F. Li, X. C. Le, *Anal. Chem.* **2009**, *81*, 7484–7489.

[9] H. Cho, B. R. Baker, S. Wachsmann-Hogiu, C. V. Pagba, T. A. Laurence, S. M. Lane, L. P. Lee, J. B.-K. Tok, *Nano Lett.* **2008**, *8*, 4386–4390.

[10] D. K. Kim, K. Kerman, H. M. Hiep, M. Saito, S. Yamamura, Y. Takamura, Y. S. Kwon, E. Tamiya, *Anal. Biochem.* **2008**, *379*, 1–7.

[11] A. Hecht, A. A. Kumar, R. Kopelman, *Anal. Chem.* **2011**, *83*, 7123–7128.

[12] a) J. Kuijt, F. Ariese, U. A. T. Brinkman, C. Gooijer, *Anal. Chim. Acta* **2003**, *488*, 135–171; b) I. Sánchez-Barragán, J. M. Costa-Fernández, M. Valledor, J. C. Campo, A. Sanz-Medel, *TrAC Trends Anal. Chem.* **2006**, *25*, 958–967.

[13] a) X. Shu, Y. Chen, H. Yuan, S. Gao, D. Xiao, *Anal. Chem.* **2007**, *79*, 3695–3702; b) Y. Li, X. Liu, H. Yuan, D. Xiao, *Biosens. Bioelectron.* **2009**, *24*, 3706–3710; c) T. Zhou, N. Wang, C. Li, H. Yuan, D. Xiao, *Anal. Chem.* **2010**, *82*, 1705–1711; d) J. Li, W. Zhou, X. Ouyang, H. Yu, R. H. Yang, W. Tan, J. Yuan, *Anal. Chem.* **2011**, *83*, 1356–1362.

[14] a) Y. He, H. F. Wang, X. P. Yan, *Anal. Chem.* **2008**, *80*, 3832–3837; b) H. F. Wang, Y. He, T. R. Ji, X. P. Yan, *Anal. Chem.* **2009**, *81*, 1615–1621; c) Y. He, H. F. Wang, X. P. Yan, *Chem. Eur. J.* **2009**, *15*,

5436–5440; d) P. Wu, Y. He, H. F. Wang, X. P. Yan, *Anal. Chem.* **2010**, *82*, 1427–1433; e) H. F. Wang, Y. Li, Y. Y. Wu, Y. He, X. P. Yan, *Chem. Eur. J.* **2010**, *16*, 12988–12994; f) H. Yan, H. F. Wang, *Anal. Chem.* **2011**, *83*, 8589–8595.

[15] a) W. J. Jin, J. M. Costa-Fernández, A. Sanz-Medel, *Anal. Chim. Acta* **2001**, *431*, 1–9; b) B. S. Vicente de La Riva, J. M. Costa-Fernández, W. J. Jin, R. Pereiro, A. Sanz-Medel, *Anal. Chim. Acta* **2002**, *455*, 179–186; c) J. Díaz-Garć, J. M. Costa-Fernández, N. Bordel, R. Pereiro, A. Sanz-Medel, *Anal. Chim. Acta* **2003**, *486*, 1–10; d) J. M. Traviesa-Alvarez, J. M. Costa-Fernández, R. Pereiro, A. Sanz-Medel, *Talanta* **2004**, *62*, 827–833.

[16] a) A. Hagfeldt, M. Graetzel, *Chem. Rev.* **1995**, *95*, 49–68; b) W. C. W. Chan, S. Nie, *Science* **1998**, *281*, 2016–2018; c) M. Nirmal, L. Brus, *Acc. Chem. Res.* **1999**, *32*, 407–414; d) M. A. El-Sayed, *Acc. Chem. Res.* **2004**, *37*, 326–333; e) A. M. Smith, S. Nie, *Acc. Chem. Res.* **2010**, *43*, 190–200.

[17] a) F. Gao, P. Cui, X. Chen, Q. Ye, M. Li, L. Wang, *Analyst* **2011**, *136*, 3973–3980; b) F. Gao, Q. Ye, P. Cui, X. Chen, M. Li, L. Wang, *Anal. Methods* **2011**, *3*, 1180–1185; c) F. Gao, Q. Ye, P. Cui, L. Zhang, *J. Agric. Food Chem.* **2012**, *60*, 4550–4558.

[18] a) R. S. Swathi, K. L. Sebastian, *J. Chem. Phys.* **2008**, *129*, 054703; b) R. S. Swathi, K. L. Sebastian, *J. Chem. Phys.* **2009**, *130*, 086101.

[19] a) H. Li, J. Zhai, X. Sun, *Langmuir* **2011**, *27*, 4305–4308; b) S. Chandra, P. Das, S. Bag, D. Laha, P. Pramanik, *Nanoscale* **2011**, *3*, 1533–1540; c) S. N. Baker, G. A. Baker, *Angew. Chem.* **2010**, *122*, 6876–6896; *Angew. Chem. Int. Ed.* **2010**, *49*, 6726–6744; d) J. Zhou, C. Booker, R. Li, X. Zhou, T. Sham, X. Sun, Z. Ding, *J. Am. Chem. Soc.* **2007**, *129*, 744–745; e) Md. P. Sk, A. Jaiswal, A. Paul, S. S. Ghosh, A. Chattopadhyay, *Sci. Rep.* **2012**, *2*, 383; f) H. Zhu, X. Wang, Y. Li, Z. Wang, F. Yang, X. Yang, *Chem. Commun.* **2009**, 5118–5120.

[20] J. Zhuang, X. Zhang, G. Wang, D. Li, W. Yang, T. Li, *J. Mater. Chem.* **2003**, *13*, 1853–1857.

[21] a) R. J. Hurtubise, A. H. Ackerman, B. W. Smith, *Appl. Spectrosc.* **2001**, *55*, 490–495; b) W. J. Jin, J. M. Costa-Fernández, R. Pereiro, A. Sanz-Medel, *Anal. Chim. Acta* **2004**, *522*, 1–8.

[22] a) C. H. Lu, H. H. Yang, C. L. Zhu, X. Chen, G. N. Chen, *Angew. Chem.* **2009**, *121*, 4879–4881; *Angew. Chem. Int. Ed.* **2009**, *48*, 4785–4787; b) R. Yang, J. Jin, Y. Chen, N. Shao, H. Kang, Z. Xiao, Z. Tang, Y. Wu, Z. Zhu, W. Tan, *J. Am. Chem. Soc.* **2008**, *130*, 8351–8358.

[23] M. J. Warwich, in *Immunoassay: A Practical Guide* (Ed.: B. Law), Taylor & Francis, Bristol, **1996**, p. 28.

[24] a) M. A. Shuman, P. W. Majerus, *J. Clin. Invest.* **1976**, *58*, 1249–1258; b) E. Heyduk, T. Heyduk, *Anal. Chem.* **2005**, *77*, 1147–1156.

Received: February 14, 2013
Published online: ■■ ▮▮, 0000

Biosensors

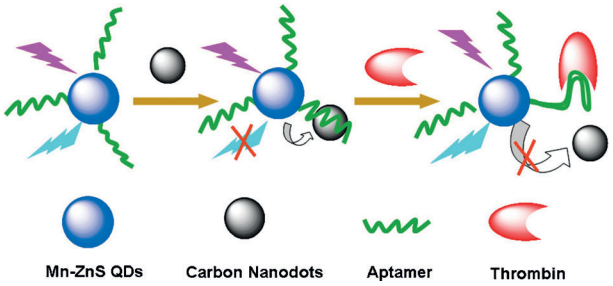

A PET biosensor: This study presents the first example of a sensitive, selective, and stable phosphorescent sensor based on phosphorescence energy transfer (PET) for thrombin that uses a thrombin–aptamer recognition event (see figure; QDs = quantum dots).